J Mater Sci (2009) 44:4191–4194
DOI 10.1007/s10853-009-3546-0

LETTER

Compressive deformation behavior of porous PLLA/PCL polymer blend

Mitsugu Todo · Joo-Eon Park · Hiroyuki Kuraoka · Jin-Woong Kim · Kentaro Taki · Masahiro Ohshima

Received: 1 April 2009 / Accepted: 4 May 2009 / Published online: 22 May 2009
© Springer Science+Business Media, LLC 2009

Biodegradable polymers such as poly(L-lactide) (PLLA) and their composite materials with bioactive ceramics such as hydroxyapatite have been considered to be used as scaffolds having a variety of porous structures for cell culture in regenerative medicine [1–9]. From a mechanical point of view, it is ideal that a scaffold have proper mechanical properties biomechanically compatible to the target tissue to be regenerated at the initial stage of implantation. It is therefore important to develop scaffolds having a wide range of mechanical properties by controlling their structures and constituents. In our previous study, we developed a porous structure of pure PLLA and its deformation mechanism under compression was discussed [10]. It was also shown that the pore size and the compressive mechanical properties can be controlled by changing the concentration of the solution. Another effective way to control the mechanical properties of such polymeric scaffolds is polymer blending in which, for example, PLLA is mixed with a ductile biodegradable polymer such as poly(ε-caplolactone) (PCL) having much lower strength and modulus than PLLA. The mechanical properties of bulk PLLA/PCL blends have been characterized in the previous studies [11–14]; however, few studies have been performed on the development and characterization of porous structures of PLLA/PCL.

In this study, porous PLLA/PCL was fabricated by using the solid–liquid phase separation method and the solvent sublimation process [5, 10, 15]. Pelletized PLLA and PCL with a mixture ratio of 80:20 were dissolved in 1,4-dioxane to prepare PLLA/PCL solution of 7 wt%. The solution was then filled into a PP tube, and frozen from the bottom part at a constant rate in liquid nitrogen to induce solid–liquid phase separation. Thereafter, the frozen samples were dried under vacuum at −5 °C for about 1 week to remove the solvent. Cylindrical specimens of 8-mm diameter and 12-mm length were then fabricated. For comparison, porous structures of pure PLLA and PCL were also fabricated using the same process. The porosity was 89% for all the materials. Compression tests of the porous specimens were conducted by using a conventional testing machine, and the compressive mechanical properties such as the critical stress and the modulus were evaluated, where the critical stress was defined as a peak stress at which the compressive stress–strain relation completed the initial linear elastic deformation behavior. The surfaces of the deformed and undeformed specimens were also observed using a field emission scanning electron microscope (FE-SEM) to characterize the porous microstructure and the deformation mechanism under compression.

FE-SEM micrographs of the vertical and longitudinal cross-sections are shown in Fig. 1. The left hand and right hand sides are the vertical and the longitudinal, respectively. Different morphologies are observed on the both cross-sections. The pores are homogeneously distributed on the vertical surfaces and the pore size of PCL is larger than that of PLLA. The largest pores existing in all the samples are thought to be created as aggregations of gas dissolved in the solutions. It is interesting to note that the

M. Todo (✉)
Research Institute for Applied Mechanics, Kyushu University, 6-1 Kasuga-koen, Kasuga 816-8580, Japan
e-mail: todo@riam.kyushu-u.ac.jp

J.-E. Park · H. Kuraoka
Interdisciprinary Graduate School of Engineering and Sciences, Kyushu University, Kasuga, Japan

J.-W. Kim · K. Taki · M. Ohshima
Department of Chemical Engineering, Kyoto University, Kyoto, Japan

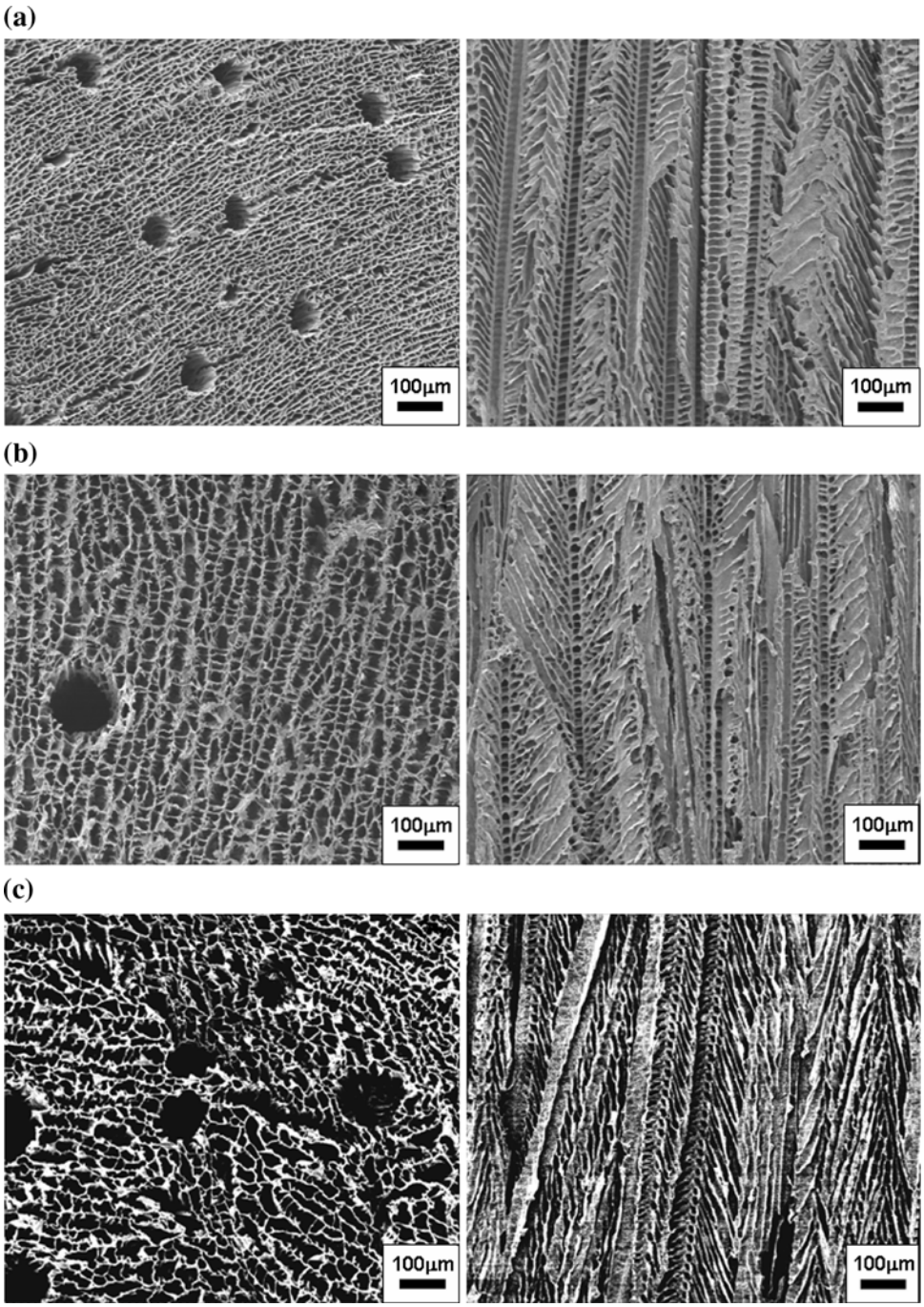

Fig. 1 FE-SEM micrographs of cross-sections. The left are the vertical cross sections and the right are the longitudinal cross sections. **a** PLLA, **b** PLLA/PCL, and **c** PCL

microstructural morphologies observed on the longitudinal sections are similar to comb pattern. Typical stress–strain curves under compression are shown in Fig. 2. For each of the curves, there is a critical point which is recognized as the end of the initial linear portion of the stress-strain relation. This critical point can also be understood microstructurally as the initiation of localized buckling deformation as shown in Fig. 3. The constant or decreasing stress portions of the stress–strain curves correspond to increase of microstructural buckling deformation. The stress starts to increase again when buckling deformation reaches saturation. The initial elastic modulus, the slope of the initial linear portion, and the critical stress values are shown in Fig. 4. It is clearly understood that these mechanical properties of PLLA/PCL stands between pure PLLA and PCL, indicating that the compressive properties

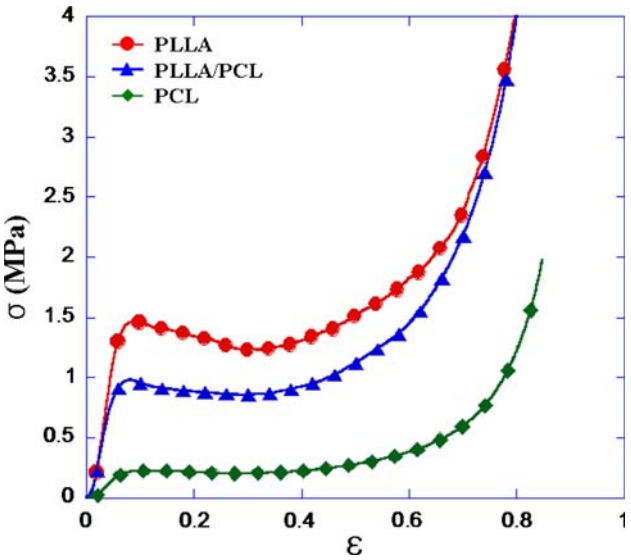

Fig. 2 Stress–strain curves under compression

of the biodegradable scaffolds can be controlled by using polymer blending.

In summary, porous structure of PLLA/PCL polymer blend was successfully fabricated by using the solid–liquid phase separation method and the subsequent solvent sublimation process. The compressive mechanical properties such as the initial elastic modulus and the critical stress were then evaluated and compared with those of porous structures of pure PLLA and PCL. The experimental results suggested that these properties can be controlled by using polymer blending with various blend ratios. The deformation mechanisms associated with the microstructures were also investigated by using FE-SEM. The critical point can be recognized as the initiation of localized buckling deformation.

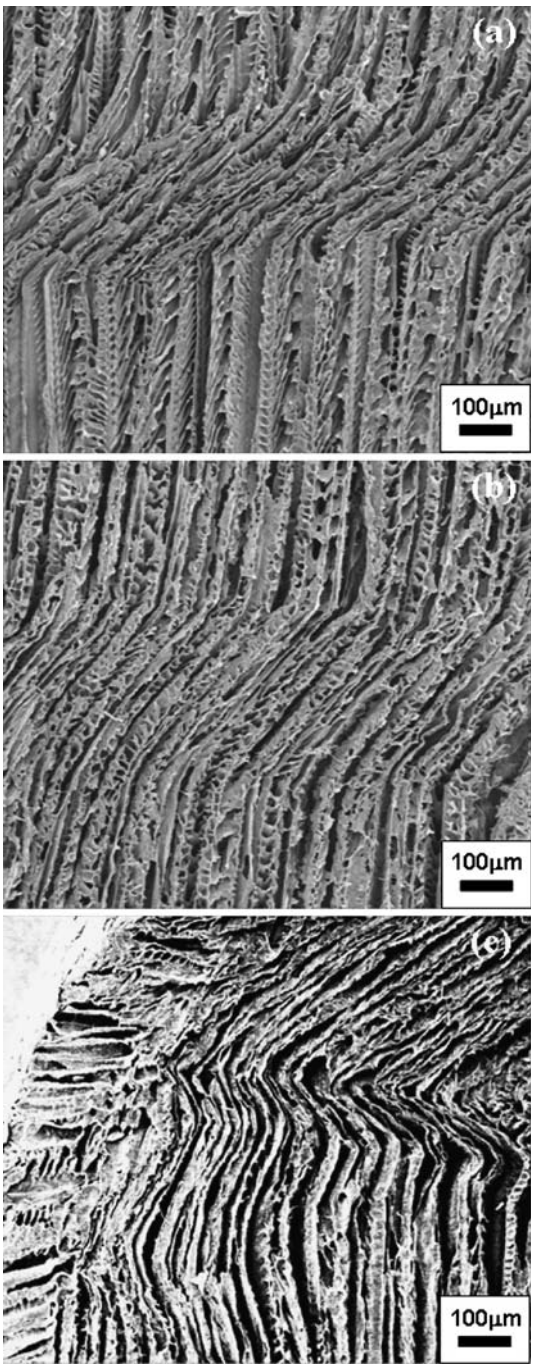

Fig. 3 Buckling behavior at critical stress. **a** PLLA, **b** PLLA/PCL, and **c** PCL

References

1. Hutmacher DW (2000) Biomaterials 21:2529
2. Mikos AG, Thorsen AJ, Czerwonka LA, Bao Y, Langer R (1993) Polymer 35:1068
3. Howard D, Partridge K, Yang X, Clarke NMP, Okubo Y, Bessho K, Howdle SM, Sharesheff KM, Oreffo OC (2002) Biochem Biophys Res Commun 299:208
4. Lin ASP, Barrows TH, Cartmell SH, Guldberg RE (2003) Biomaterials 24:481
5. Zhang R, Ma PX (1999) J Biomed Mater Res 44:446
6. Ma PX, Zhang R, Xiao G, Franceschi (2001) J Biomed Mater Res 54:284
7. Wei G, Ma PX (2004) Biomaterials 25:4749
8. Teng X, Ren J, Gu S (2007) J Biomed Mater Res Part B 81B:185
9. Georgiou G, Mathieu L, Pioletti DP, Bourban PE, Manson JAE, Knowles JC, Nazhat SN (2007) J Biomed Mater Res Part B 80B:322
10. Todo M, Kuraoka H, Kim JW, Taki K, Ohshima M (2008) J Mater Sci 43(16):5644. doi:10.1007/s10853-008-2881-x
11. Takayama T, Todo M (2006) J Mater Sci 41:4989. doi:10.1007/s10853-006-0137-1
12. Takayama T, Todo M, Tsuji H, Arakawa K (2006) J Mater Sci 41:6501. doi:10.1007/s10853-006-0611-9
13. Todo M, Takayama T, Tsuji H, Arakawa K (2007) J Solid Mech Mater Eng 1:1157
14. Todo M, Park SD, Takayama T, Arakawa K (2007) Eng Frac Mech 74:1872
15. Kim JK, Taki K, Nagamine S, Ohshima M (2008) Chem Eng Sci 63:3858

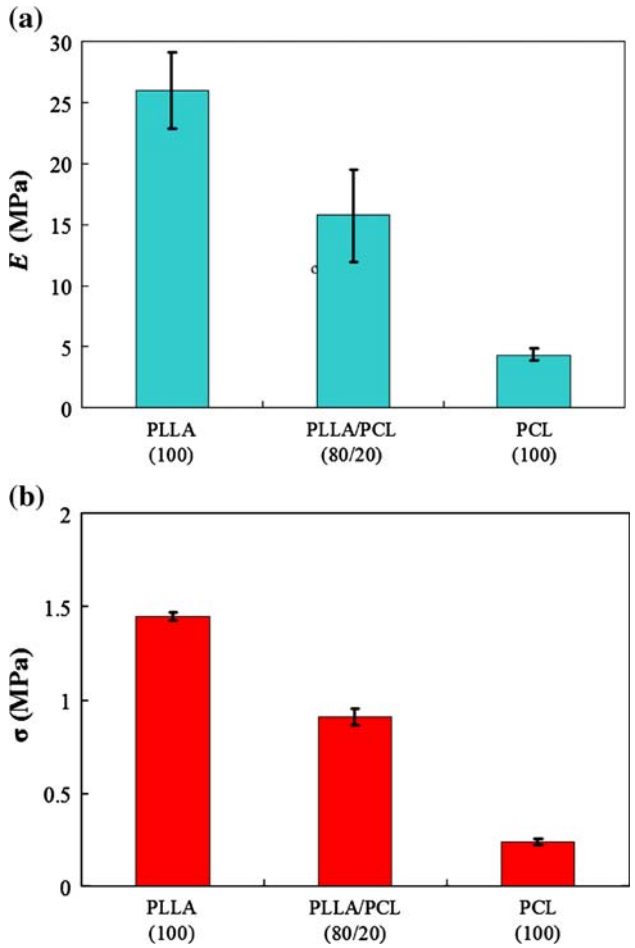

Fig. 4 Compressive mechanical properties. **a** Initial elastic modulus, **b** Critical stress